Molecular Biology of the Cell
Vol. 11, 201–215, January 2000

The Rib43a Protein Is Associated with Forming the Specialized Protofilament Ribbons of Flagellar Microtubules in *Chlamydomonas*

Jan M. Norrander, Aimee M. deCathelineau,* Jennifer A. Brown, Mary E. Porter, and Richard W. Linck†

Department of Genetics, Cell Biology, and Development, University of Minnesota, Minneapolis, Minnesota 55455

Submitted April 21, 1999; Revised September 30, 1999; Accepted October 22, 1999
Monitoring Editor: J. Richard McIntosh

Ciliary and flagellar microtubules contain a specialized set of three protofilaments, termed ribbons, that are composed of tubulin and several associated proteins. Previous studies of sea urchin sperm flagella identified three of the ribbon proteins as *tektins*, which form coiled-coil filaments in doublet microtubules and which are associated with basal bodies and centrioles. To study the function of tektins and other ribbon proteins in the assembly of flagella and basal bodies, we have begun an analysis of ribbons from the unicellular biflagellate, *Chlamydomonas reinhardtii*, and report here the molecular characterization of the ribbon protein rib43a. Using antibodies against rib43a to screen an expression library, we recovered a full-length cDNA clone that encodes a 42,657-Da polypeptide. On Northern blots, the rib43a cDNA hybridized to a 1.7-kb transcript, which was up-regulated upon deflagellation, consistent with a role for rib43a in flagellar assembly. The cDNA was used to isolate *RIB43a*, an ~4.6-kb genomic clone containing the complete rib43a coding region, and restriction fragment length polymorphism analysis placed the *RIB43a* gene on linkage group III. Sequence analysis of the *RIB43a* gene indicates that the substantially coiled-coil rib43a protein shares a high degree of sequence identity with clones from *Trypanosoma cruzi* and *Homo sapiens* (genomic, normal fetal kidney, and endometrial and germ cell tumors) but little sequence similarity to other proteins including tektins. Affinity-purified antibodies against native and bacterially expressed rib43a stained both flagella and basal bodies by immunofluorescence microscopy and stained isolated flagellar ribbons by immuno-electron microscopy. The structure of rib43a and its association with the specialized protofilament ribbons and with basal bodies is relevant to the proposed role of ribbons in forming and stabilizing doublet and triplet microtubules and in organizing their three-dimensional structure.

INTRODUCTION

Cilia and flagella perform essential motile, sensory, and developmental functions in organisms from protists to humans. These organelles function in the propulsion of cells and in the transport of extracellular substances, such as water-borne food particles, and cerebrospinal, embryonic, oviduct, and tracheal fluids. Nonmotile cilia are also present in sensory cells, such as retinal photoreceptors, auditory hair cells, and chemo-, mechano-, and olfactory receptors (Wheatley, 1982; Perkins *et al.*, 1986; Keil, 1997). Several sensory and behavioral mutants of *Caenorhabditis elegans* have been identified with defects in the assembly of sensory cilia (Perkins *et al.*, 1986; Collet *et al.*, 1998). In humans, motile cilia are affected in Kartagener's syndrome, a disease associated with chronic respiratory distress, male sterility, and situs inversus (Afzelius, 1995; Srivastava, 1997). Finally, in transgenic mice, after the homozygous knockout of the kinesin KIF3B gene, the absence of embryonic cilia leads to the disruption of normal left–right asymmetry, defects in heart development, and other abnormalities (Nonaka *et al.*, 1998; see also Chen *et al.*, 1998; Mochizuki *et al.*, 1998). The mechanism of ciliary and flagellar assembly, therefore, has

* Present address: B216 Pathology, University of Colorado Health Sciences Center, Denver, CO 80262.
† Corresponding author. E-mail address: linck@lenti.med.umn.edu.
Abbreviations used: EM, electron microscopy; EST, expressed sequence tag; IgG, immunoglobulin G; IPTG, isopropyl-1-thio-β-D-galactopyranoside; rib43a, the wild-type 42,657-Da polypeptide; *RIB43a*, the gene for rib43a; rib43aNΔ64, the rib43a polypeptide lacking the N-terminal 64 amino acids; RT, room temperature; TBS, Tris-buffered saline; TBST, TBS and Tween 20.

important consequences for both the development and viability of organisms.

Most cilia, flagella, basal bodies, and centrioles are constructed from an evolutionarily conserved, ninefold arrangement of doublet or triplet microtubules, the axoneme (Gibbons, 1981). Doublet and triplet microtubules are highly stable, chemically complex, and structurally asymmetric polymers (Tilney *et al.*, 1973; Piperno *et al.*, 1977; Linck, 1990; Dutcher, 1995; Dutcher and Trabuco, 1998). In particular the A-microtubule provides sites for the assembly of the B-tubule, the highly complex arrangement of centriolar linkages, and the attachment sites for ciliary and flagellar dynein arms, radial spokes, and nexin links (Gibbons, 1981; Goodenough and Heuser, 1985; Mastronarde *et al.*, 1992). However, little is known about the proteins and mechanisms that are involved in the assembly and stability of these conserved microtubules.

The three-dimensional arrangement of axonemal components is determined by the template function of the basal body and by information residing in the A-microtubule. The nature of the basal body template is not known, but studies of flagellar doublet microtubules provide some clues. For example, in reconstitution experiments, purified outer dynein arms (Gibbons and Gibbons, 1979; Takada and Kamiya, 1994) and inner arms (Smith and Sale, 1992) rebind to their unique locations on the A-tubules. Other components of the axoneme also bind along the A-tubules with complex axial spacings that are multiples of the 8-nm tubulin dimer repeat, suggesting the presence of longitudinal molecular rulers. Outer dynein arms, each composed of two to three heavy chains and associated intermediate and light chains (Witman *et al.*, 1994; Fowkes and Mitchell, 1998), repeat at 24 nm in a single row along the length of the axoneme (Allen and Borisy, 1974; Warner and Satir, 1974), the axial spacing being an inherent property of outer arms (Haimo *et al.*, 1979). Inner dynein arms have a more complex chemical composition and axial subspacing, with an overall 96-nm repeat (Goodenough and Heuser, 1985a,b; Mastronarde *et al.*, 1992); in vivo, specific inner arm isoforms assemble with these periodicities, even in mutants lacking other adjacent, heterologous inner arm isoforms (Piperno *et al.*, 1990). The arrangement of radial spokes is also complex and species specific, with spokes occurring in pairs in *Chlamydomonas* but in triplets in many other organisms (e.g., *Tetrahymena*, sea urchin, and rat), in all cases with an axial repeat of 96 nm (Gibbons, 1981; Goodenough and Heuser, 1985b). Finally, the nexin links also repeat at 96-nm intervals (Gibbons, 1981), connecting the cylinder of nine A-microtubules in some species (cf. Stephens *et al.*, 1989). Even though these components all interact with the A-microtubule surface lattice (Amos and Klug, 1974), it seems likely that the three-dimensional complexity of the A-tubule arises from accessory proteins besides tubulin, given that the flagellar axoneme of at least one species (e.g., *Chlamydomonas*) is constructed from a single dimer isoform of $\alpha\beta$-tubulin (Silflow *et al.*, 1985; James *et al.*, 1993).

Our interest in this problem is in the role of a specialized set of three protofilaments of flagellar microtubules. These protofilaments are resistant to solubilization by Sarkosyl detergent and have the appearance of ribbons by negative stain electron microscopy (EM) (Meza *et al.*, 1972; Witman *et al.*, 1972ab). Ribbons contain a longitudinal filament composed of the fibrous proteins *tektins* and associated proteins (Linck, 1990; Hinchcliffe and Linck, 1998). The molecular biology of tektins has so far been studied in detail in sea urchin sperm flagella and embryonic cilia and in mouse testis, resulting in the identification of a gene family, so far including tektins A $\cong$ 53-kDa, B $\cong$ 51-kDa, and C $\cong$ 47-kDa (Norrander *et al.*, 1992, 1995, 1996, 1998; Chen *et al.*, 1993). The structural properties and locations of tektins in the A-tubule suggest they may function as templates and rulers in generating the three-dimensional organization of the axoneme (Linck, 1990; Pirner and Linck, 1994; Nojima *et al.*, 1995; Norrander *et al.*, 1996).

To understand the specific role of these accessory proteins in flagellar assembly, we have turned to the model system of *Chlamydomonas reinhardtii*, a unicellular, biflagellate green alga that is accessible both to the genetic analysis of mutant motility phenotypes and to the biochemical and structural analyses of isolated flagella (Piperno and Luck, 1977; Huang *et al.*, 1979; Dutcher, 1986; Nelson *et al.*, 1994; Witman *et al.*, 1994; Porter, 1996). Numerous mutants have been isolated that affect the assembly and/or function of basal bodies or flagella (Harris, 1989). We report here the cloning and characterization of the first ribbon protein/gene, rib43a/*RIB43a*, from *Chlamydomonas*, and discuss the potential function of rib43a in flagellar and basal body microtubules.

MATERIALS AND METHODS

Isolation of Axonemes and Ribbons from Chlamydomonas

Unless specified otherwise, the procedures were conducted at 4°C, and centrifuges and rotors refer to those of Beckman Instruments (Schaumburg, IL). *Chlamydomonas reinhardtii* wild-type vegetative cells (strain *137C*) were grown to a density of 1–2 $\times$ 10^6 cells/ml in rich medium containing sodium acetate and additional potassium phosphate as described by Witman (1986) and King *et al.* (1986), as modified by Gardner *et al.* (1994). For the isolation of axonemes, 20- to 40-l cultures were concentrated to 1-l by tangential flow at room temperature (RT) using a Pellicon HVMP-000C5 0.45-μm filter (Millipore, Bedford, MA), followed by centrifugation in a JA14 rotor at 1200 rpm x 5 min. Cells were resuspended and consolidated to 200 ml in HEPES buffer (10 mM HEPES, pH 7.5, 1 mM $SrCl_2$, 4% sucrose, 1 mM DTT) and deflagellated by pH shock (Witman *et al.*, 1972a). Flagella were isolated and demembranated using previously published procedures (Gardner *et al.*, 1994). To isolate ribbons, axoneme pellets were resuspended in 0.7% Sarkosyl in TED (10 mM Tris, pH 8, 0.1 mM EDTA, 1 mM DTT), incubated overnight, and pelleted in an Optima TLX ultracentrifuge at 100,000 $\times$ *g* for 1 h. Pellets of ribbons were washed once by resuspending in 1 ml of TED and recentrifuging.

SDS-PAGE and Blotting

Protein samples were resuspended in 1$\times$ SDS media (electrophoresis grade SDS; Bio-Rad, Hercules, CA) buffer, incubated at 37°C for 30 min, boiled for 5 min, and loaded onto polyacrylamide gels (Laemmli, 1970). Stacking gels were 3% acrylamide from a stock solution of 30:0.8% acrylamide:bisacrylamide (Bio-Rad); resolving gels were 7.5% acrylamide. Proteins were blotted to nitrocellulose (Schleicher & Schuell, Keene, NH) in 10 mM 3-[cyclohexylamino]-1-propanesulfonic acid, pH 11, 10% methanol, at 60 mA for 2 h at 4°C. Transferred proteins were stained with 0.02% Ponceau S (Sigma, St. Louis, MO) in 3% trichloroacetic acid.

Antibody Production and Affinity Purification

Rabbit antibodies were raised against the rib43a axonemal ribbon protein from *Chlamydomonas* (anti-rib43a) and against its bacterially expressed form, rib43aΔN64 (anti-rib43aΔN64). For anti-rib43a, 0.25- to 0.75-mg ribbons from *Chlamydomonas* was resolved by SDS-PAGE (0.75 mm thick × 13 cm wide × 15 cm tracking dye migration distance), blotted to nitrocellulose, and stained with 0.02% Ponceau S. The band containing the protein of interest (~100 μg) was excised. The nitrocellulose strip was dried, dissolved in DMSO, mixed 1:1 with complete Freund's adjuvant, and injected subcutaneously into a 4-kg female White New Zealand rabbit. A second, booster injection was given after 21 d, using a second protein-nitrocellulose strip dissolved in DMSO and mixed 1:1 with incomplete Freund's adjuvant. Whole sera were isolated 2 wk after the booster injection and tested for staining of rib43a protein on immunoblots of *Chlamydomonas* axonemes.

Subsequently, this same procedure was used to raise antibody against the initial β-galactosidase fusion protein (anti-rib43aΔN64). The cDNA clone pBrib43aΔN64 was used to express a 39-kDa fusion protein consisting of the first 37 amino-terminal residues of β-galactosidase (coded for by the pBluescript cloning vector; Stratagene, La Jolla, CA) and the 303 amino acid residues of rib43aΔN64 (see Bacterial Expression and Isolation of Fusion Proteins). Isopropyl-1-thio-β-D-galactopyranoside (IPTG)-induced fusion protein contained in bacterial inclusion bodies was resolved by SDS-PAGE and transferred to nitrocellulose. Strips of nitrocellulose were probed with anti-rib43a, which stained the induced protein. The protein band so identified was excised and treated as above to produce rabbit antisera, i.e., anti-rib43aΔN64.

For use in Western blotting, immunofluorescence microscopy, and immuno-EM, anti-rib43a and anti-rib43aΔN64 antibodies were affinity purified as follows: 1) 5 mg of His-tagged rib43a protein (expressed in pET; see Bacterial Expression and Isolation of Fusion Proteins) was coupled to 0.5 ml of cyanogen bromide-activated Sepharose 4B, according to the manufacturer's recommended procedures (Sigma). 2) The 0.5-ml column bed was washed with 10 ml of sterile PBS. 3) 0.5 ml of serum was applied and incubated for 30 min. 4) The column was washed with 16 ml of PBS. 5) Specific, bound antibody was eluted with 0.2 M glycine, pH 3.0, and collected in 0.5-ml fractions containing 0.07 ml 1 M Tris base. 6) The 0.5-ml peak fraction (OD at 280 nm) was diluted with 0.5 ml of blocking buffer (5% normal serum, 1% fish gelatin, 5% glycerol in Tris-buffered saline [TBS; 20 mM Tris, pH 7.5, 0.5 M NaCl]) and dialyzed against TBS. 7) The dialyzed sample was further diluted with 0.5 ml of blocking buffer and stored at 4°C.

Immunoblot Analysis

Nitrocellulose blots were blocked with 3% BSA in TBS at RT (unless specified otherwise) for 1 h. Primary antibodies were diluted into 1% BSA-TBST (TBS + 0.05% Tween). Blots were incubated with primary antibody for 2 h, followed by three 10-min washes with 0.1% BSA-TBST. Blots were incubated with alkaline phosphatase-conjugated, goat anti-rabbit immunoglobulin G (IgG; Pierce, Rockford, IL), diluted into 1% BSA-TBS, for 2 h. This secondary antibody step was followed by three 10-min washes with 0.1% BSA-TBST. Substrate solution consisted of the following formulation: 15 ml of buffer (0.1 M NaCl, 5 mM $MgCl_2$, 0.1 M Tris, pH 9.5), 0.05 ml of 50 mg/ml nitroblue tetrazolium in 70% dimethylformamide, and 0.1 ml of 50 mg/ml 5-bromo-4-chloro-3-indoyl phosphate in 100% dimethyformamide. Blots were incubated in substrate solution until bands appeared (1–3 min) and then washed with an excess of ice-cold distilled H_2O.

Isolation and Sequencing of cDNA and Genomic Clones

A λZapII cDNA expression library, constructed from transcripts isolated from strain *1132D−*, 30 minutes after deflagellation (Wilkerson *et al.*, 1994), was screened with anti-rib43a antibody using standard procedures (Young and Davis, 1983). A cDNA containing a partial coding sequence (subsequently termed clone pBrib43aΔN64) was isolated. The library was rescreened with radiolabeled pBrib43aNΔ64 (Sambrook *et al.*, 1989) to obtain a clone containing the complete coding sequence (pBrib43a).

A λ genomic library, constructed in λFIX II (Stratagene) from the wild-type strain *21gr* (Schnell and Lefebvre, 1993), was screened with the cDNA clone pBrib43a, using standard methods (Sambrook *et al.*, 1989). Eleven overlapping clones were isolated and restriction mapped. A 4634-bp *Hin*dII fragment, shown by Southern blot analysis (Southern, 1975) to contain the entire pBrib43a cDNA sequence, was subcloned into pBluescript SK(−) to produce the genomic clone pRIB43a, containing the gene for the *C. reinhardtii* ribbon 43-kDa polypeptide, rib43a.

Sequence Analysis

The sequencing of pBrib43aΔN64, pBrib43a and pRIB43a was carried out by the DNA Sequencing and Synthesis Facility, Iowa State University (Ames, IA). Sequence assembly and analysis were performed using the Genetics Computer Group (Madison, WI) Wisconsin Software Package, version 9.1. Database searches were performed using BLAST (Altschul *et al.*, 1990). Tertiary structure predictions were made using CoilScan (Lupas *et al.*, 1991; Lupas, 1996). Multiple-sequence alignments were performed using PileUp (Genetics Computer Group). In calculations of homologies and similarities, the following residues were considered to be conservative substitutions: D and E (acidic, negatively charged); H, K, and R (basic, positively charged); A, F, I, L, M, V, and Y (hydrophobic, nonpolar); and S and T (possible phosphorylation sites).

Copy Number and Mapping of the RIB43a Clone

To determine the number of gene copies, DNA was isolated from wild-type strain *137C*, digested with *Xho*I, *Sac*I, and *Hin*dIII, and analyzed by Southern blots using the cDNA clone pBrib43a as a probe. To place the *RIB43a* gene on the genetic map, the genomic clone pRIB43a was used to probe a series of mapping filters (*Eco*RI–*Xho*I digests), as previously described by Porter *et al.* (1996).

Bacterial Expression and Isolation of Fusion Proteins

The β-galactosidase-rib43aΔN64 fusion protein was expressed in pBluescript SK(−), using the original clone isolated by antibody screening of the λZapII cDNA library. XL1-Blue MRF cells transformed with pBrib43aΔN64 were grown in Luria–Bertani media with 150 μg/ml ampicillin and 12.5 μg/ml tetracycline for 4 h at 37°C with shaking. IPTG (1 mM) was added to induce expression, and the incubation continued overnight. Cells were pelleted at 500 x *g* for 15 min at 4°C. Each gram of cells was resuspended in 3 ml of lysis buffer (50 mM Tris, pH 8, 1 mM EDTA, 10 mM NaCl), 4 μl of 50 mM PMSF, 80 μl of lysozyme (10 mg/ml), and 4 mg of deoxycholic acid. Resuspended cells were sonicated three times for 10 s on ice. DNA was digested with the addition of 20 μl of DNase I (1 mg/ml) followed by a 30-min incubation at 37°C. Inclusion bodies were pelleted at 17,500 x *g* (12,000 rpm in a JA-20 rotor) for 15 min at 4°C and resuspended in 1.5 ml of lysis buffer plus 0.5% Triton X-100; the insoluble protein fraction was pelleted as before. Pellet proteins were resuspended in 1× SDS buffer (2% SDS [electrophoresis grade, Bio-Rad, Hercules, CA], 192 mM glycine, 25 mM Tris, pH 6.8, 15% glycerol, 0.02% bromphenol blue, 20 mM dithiothreitol, 10% β-mercaptoethanol), incubated at 37°C for 30 min, boiled for 5 min, resolved by SDS-PAGE, and transferred to nitrocellulose. The strips were stained with Ponceau S and with anti-rib43a antibody; the protein band, which was induced by IPTG and recognized by anti-rib43a, was used to raise rabbit polyclonal antibodies, i.e., anti-rib43aΔN64, as described previously.

A second expression plasmid was constructed to produce a His-tagged rib43a protein. An *Nde*I site was introduced into the pBrib43a sequence at the initiation codon, using oligonucleotide-directed mutagenesis (Norrander *et al.,* 1983) to produce the clone pBrib43aNdeI. The *Nde*I–*Xho*I fragment from this clone (containing the entire coding region and 3′ untranslated region of rib43a) was isolated from a low-melting-point agarose gel and ligated into pET-28a(+) to produce the His-tagged rib43a-expressing clone pETrib43a. This clone codes for a protein consisting of the 20-amino-acid peptide MGSSHHHHHHSSGLVPRGSH (His tag) followed by the 367 amino acids of the rib43a protein. pETrib43a was transformed into the host BL21(DE3)pLysS (Novagen, Madison, WI) for expression. Colonies were picked immediately after transformation and used to inoculate 50 ml of Luria–Bertani media containing 30 μg/ml kanamycin and 34 μg/ml chloramphenicol. Interestingly, colonies picked from the same plates as little as 1 d later or colonies restreaked onto fresh plates failed to produce any His-rib43a protein when cultured and induced. Cultures were incubated with shaking at 37°C until reaching an OD_{600} of ~0.6. IPTG was added to a concentration of 1 mM, and the incubation continued for 4 h. Cells were harvested by centrifugation at 5000 x *g* for 5 min at 4°C, and the cells were lysed by freezing and thawing. Thawed cells were resuspended in 4 ml of cold 1× binding buffer (5 mM imidazole, 0.5 M NaCl, 20 mM Tris, pH 7.9) and sonicated four times for 10 s on ice. Cell debris was pelleted by centrifugation at 39,000 x *g* for 20 min at 4°C. The supernatant fraction was passed through a 0.45-μm membrane filter and loaded onto a column of Ni^{2+} immobilized on His·Bind metal chelation resin (Novagen). The column was washed with 60 mM imidazole, 0.5 M NaCl, 20 mM Tris, pH 7.9, and eluted with 1 M imidazole, 0.5 M NaCl, 20 mM Tris, pH 7.9. Protein containing fractions were dialyzed into 1× binding buffer overnight at 4°C.

RNA Isolation and Northern Blot Analysis

Total RNA was isolated before and 30 min after deflagellation by pH shock. Poly(A)$^+$ RNA was isolated by oligo(dT)-cellulose chromatography (Aviv and Leder, 1972), fractionated (5 μg/lane) on 1.5% agarose gels containing 2.2 M formaldehyde (Sambrook *et al*., 1989), and transferred to Magna Graph (Micron Separations, Westborough, MA) by capillary elution with 20× SSC, pH 7. Blots were dried and cross-linked using a UV Stratalinker. Prehybridization and hybridization solutions and conditions were as described by Myster *et al.* (1997). DNA probes were isolated from low-melting-point agarose gels, labeled with [^{32}P]dCTP using the Rediprime DNA labeling system (Amersham, Arlington Heights, IL), and added to the hybridization solution at a concentration of 1–2 × 10^6 cpm/ml. Blots were washed in 2× SSC, 0.1% SDS at RT and 0.1× SSC, 0.1% SDS at 65°C.

Immunofluorescence Microscopy

Slides or coverslips were precoated with poly-L-lysine (1 mg/ml for 30 min). Specimens (cell wall-less strain *CW92*) were applied to coated slides and slips at 2 × 10^5 cells/ml and immediately fixed by one of three procedures: 1) by plunging glass-attached live cells into methanol cooled on dry ice; 2) by briefly rinsing attached cells with HEMK (50 mM HEPES, pH 7.5, 3 mM EGTA, 1 mM $MgSO_4$, 25 mM KCl, 0.02% Na azide), followed by 5 min of incubation in 1% Nonidet NP-40 in HEMK, followed by methanol fixation; or 3) by brief rinse with HEMK, followed by 5 min of incubation in Nonidet-HEMK, followed by 30 min incubation in 2.4% paraformaldehyde in HEMK, followed by methanol fixation.

Fixed specimens were then processed in the following order: 1) incubation in blocking buffer, 1 h, 4°C; 2) incubation in buffer alone (TBST) or primary antibody in TBST, 2 h, RT; 3) four 10-min washes with TBST at RT; 4) incubation in secondary antibody in TBST, 2 h, RT; 5) four 10-min washes with TBST at RT; incubation in DAPI (4 μg/ml), 5 min, RT; deionized water wash, 5 min, RT; and 6) mounting with fluorescence antifade reagent (prepared as follows: 6 g of glycerol, 12 ml of Tris, pH 8.5, 6 ml of H_2O, 2.4 g of polyvinyl alcohol, heated to 90°C, cooled to 25°C, plus 24 mg of ρ-phenylenediamine).

Antisera and antibodies were used at the following concentrations and dilutions: anti-rib43a antibody, affinity purified with pET-expressed rib43, 1:3 dilution from column; anti-rib43aΔN64 antibody, affinity purified with pET-expressed rib43a, 1:3 dilution; mouse monoclonal 8-E11 anti-acetylated α-tubulin (Steffen *et al.*, 1994), dilution 1:100–1:250 of culture supernatant; Texas Red-conjugated goat anti-rabbit IgG (T-2767; Molecular Probes, Eugene, OR), dilution 1:200 from manufacturer's stock; and Texas Red-conjugated goat anti-mouse IgG (T-862; Molecular Probes), dilution 1:200 from manufacturer's stock. Specimens were examined using an Olympus (Tokyo, Japan) BH-2 microscope with a Zeiss (Thornwood, NY) Planapo 63×, numerical aperture 1.4 objective lens; images were photographed on Eastman Kodak (Rochester, NY) TMAX film with exposures ranging from 0.5 to 2 min.

Electron Microscopy

Negative stain and immuno-EM were conducted as previously described (Linck *et al*., 1985; Hinchcliffe and Linck, 1998). Solutions were as follows: blocking solution (0.5% cytochrome *c*, 1% fish gelatin in TED); whole preimmune serum (before immunization with rib43a); whole immune anti-rib43a serum; anti-rib43a antibody, affinity purified with pET-expressed rib43a; anti-rib43aΔN64 antibody, affinity purified with pET-expressed rib43a; and 5-nm colloidal gold-conjugated goat anti-rabbit IgG (catalogue number 15725; Ted Pella, Redding, CA). To quantitate the immunogold labeling and to assess nonspecific background and staining (Table 1), the following conditions were examined, including intermediate washes with TED as previously described: 1) control: no sample (i.e., only the blocking solution), followed by 1:200 primary antibody (affinity-purified rabbit anti-rib43aΔN64 IgG), followed by 1:50 secondary antibody (Au-goat anti-rabbit IgG); 2) control: no sample, blocking solution, zero primary antibody, 1:50 secondary antibody; 3) control: ribbon sample, blocking solution, zero primary antibody, 1:50 secondary antibody; 4) experimental: ribbon sample, blocking solution, 1:500 primary antibody, 1:200 secondary antibody; and 5) experimental: ribbon sample, blocking solution, 1:200 primary antibody, 1:200 secondary antibody. Negative staining was performed using 1% uranyl acetate. Specimens were examined, and micrographs were taken using a JEOL (Tokyo, Japan) 100CX electron microscope, operated at 80 kV.

For quantitation of immunogold labeling (for Table 1), the 5-nm gold–antibody colloid was highly monodisperse, with only four clusters of five to seven particles unattached to specimen. Three categories of gold particles were counted. 1) Particles were considered to label if they were <23 nm from the ribbons and fibrils, i.e., the distance spanned by a rabbit IgG–goat IgG complex. The labeling of ribbons and fibrils were not counted separately, because it was not always possible to distinguish between ribbons, frayed ribbons, ribbons lying on their edges, or fibrils. The numbers of gold particles appearing at the ends of ribbons and fibrils were calculated as a percentage of the total particles labeling. (2) Particles that were >23 nm from ribbons and fibrils were considered unbound. (3) Unassigned particles included ones that were positioned over unrecognizable material or near the edge of the field, where it could not be determined whether they were bound or unbound to ribbons and fibrils lying outside the field of view. For each control sample, 6–15 fields (EM negatives) were counted (~10.8 μm^2 per field at 25,000× magnification); for experimental samples, 10–15 fields were counted (~7.5 μm^2 per field at 30,000×). Finally, the data were normalized by calculating the number of particles per square micrometer × 100.

PCR of bld2 and pf5 Genomic DNA

Chlamydomonas DNA was isolated as described by Porter *et al.* (1996). Primer pairs were designed using MacVector (Oxford Molecular Group, Oxford, England) to produce ~500-bp products. A RoboCycler Gradient 96 temperature cycler (Stratagene) was used to carry out the reactions. Reactions were carried out using an Expand high-fidelity PCR system (Boehringer Mannheim, Indianapolis, IN), 0.4 μg of genomic DNA, 0.66 μg of each primer, 2 mM dNTPs, and 4% (vol/vol) DMSO. Reaction cycles were as follows: one cycle at 94°C for 3 min, 51°C for 1 min, and 74°C for 3 min; 29 cycles at 94°C for 1 min, 51°C for 1 min, and 74°C for 3 min; and one cycle at 94°C for 1 min, 51°C for 2 min, and 74°C for 5 min. PCR products were purified from 1.5% agarose gels using a Prep-A-Gene purification kit (Bio-Rad) or directly from reaction mixtures using a QIA Quick PCR purification kit (Qiagen, Valencia, CA).

RESULTS

Isolation and Cloning of Rib43aΔN64 and Rib43a

Purified *Chlamydomonas* flagellar axonemes were extracted with 0.7% Sarkosyl detergent. This treatment solubilizes most axonemal microtubule structures and associated components and yields a sedimentable fraction consisting of homogeneous, three-protofilament ribbon-like structures, similar to the ribbons derived from sea urchin sperm flagella (Linck, 1990). The appearance and homogeneity of the *Chlamydomonas* ribbons preparations are described later in EM of Ribbons and Localization of Rib43a (cf. Figure 8A). The protein composition of *Chlamydomonas* ribbons, as determined by SDS-PAGE fractionation, consists of α- and β-tubulin plus several other polypeptides in lesser amounts (Figure 1A). We chose to focus on a polypeptide, rib43a, because of its similarity in size and relative amount to tektins in sea urchin ribbons. For the purpose of molecular cloning, we tested our previously characterized sea urchin tektin antibodies (Steffen and Linck, 1988, 1989; Steffen *et al.*, 1994) and cDNAs (Norrander *et al.*, 1992, 1996; Chen *et al.*, 1993), but their cross-reactions and hybridizations on blots of *Chlamydomonas* were too weak to be useful for cloning. Consequently, we raised new polyclonal antibodies against SDS-PAGE-purified *Chlamydomonas* rib43a protein from isolated ribbon preparations. Because of the limiting yield of ribbons, the antibodies were first characterized on Western blots of *Chlamydomonas* axonemes (Figure 1B). The preimmune serum was tested and found to be negative for *Chlamydomonas* axonemal antigens. Both the anti-rib43a antisera and the affinity-purified anti-rib43a antibodies specifically recognized a single band at the position of rib43a.

The anti-rib43a antibody was used to screen a λZapII expression library constructed from wild-type RNA isolated 30 min after deflagellation (Wilkerson *et al.*, 1994), when flagellar transcripts are highest during flagellar regeneration (Lefebvre, 1995). From this screen, clone pBrib43aΔN64 was isolated, containing a 1341-bp cDNA termed rib43aΔN64, which lacks the coding region for the N-terminal 64 amino acids (see below). This clone hybridizes to a 1.7-kb transcript, which is up-regulated upon deflagellation (Figure 2), indicating that it codes for a protein involved in flagellar structure or assembly. pBrib43aΔN64 was used to rescreen the λZapII library, and a 1612-bp clone, called pBrib43a, was isolated. The largest open reading frame of pBrib43a codes for a 367-amino-acid protein with a molecular mass of 42,638 Da. The sequence of the insert in pBrib43aΔN64 was found to be identical to its corresponding sequence in pBrib43a. Several other clones with shorter inserts were also obtained by screening with the anti-rib43a antibody and with pBrib43aΔN64; however, all of them were identical in sequence with various stretches of the full-length insert of pBrib43a.

Cross-Reactivity of Antibodies Confirm Clonal Identity

The apparent molecular weight of the *Chlamydomonas* wild-type protein rib43a, as determined by SDS-PAGE (Laemmli, 1970), is ~46,000, whereas the molecular weight of the predicted protein sequence of our cloned cDNA insert from pBrib43a is 42,638 (a similar difference was observed with sea urchin tektin A_1; Norrander *et al.*, 1992). Because of this apparent difference, and because immunoscreening of libraries can result in false-positives, we sought to verify the identity of our cDNA clones. Because the full-length cDNA clone pBrib43a did not express well in initial tries with the pET system, we expressed the partial-length clone pBrib43aΔN64 (in Bluescript) to obtain a 39-kDa fusion protein, consisting of the first 37 amino-terminal residues of β-galactosidase and the 303 carboxyl-terminal amino acids of rib43a; polyclonal antibodies were raised against this rib43aΔN64 fusion protein. After our initial characterization of the anti-rib43aΔN64 antisera, we devised ways to obtain full-length rib43a expressed in pET (for explanation, see MATERIALS AND METHODS). The anti-rib43aΔN64 antisera cross-reacted on Western blots with the bacterially expressed, full-length rib43a protein from pETrib43a. We then used the expressed full-length rib43a protein as an affinity probe to purify anti-rib43a and anti-rib43aΔN64 antibodies.

The results with these affinity-purified polyclonal antibodies are as follows: 1) both the anti-rib43a antibodies (against the original wild-type flagellar protein) and the anti-rib43aΔN64 antibodies (against the truncated, bacterial expression protein) cross-reacted with the bacterial fusion proteins on Western blots (Figure 3A); 2) on blots of *Chlamydomonas* axonemes, both types of antibodies cross-reacted with the wild-type ribbon protein band, i.e., riba43a (Figures 1B and 3B); and 3) finally, on blots the anti-rib43aΔN64 antibodies cross-reacted with a single band, i.e., the wild-type rib43a protein that was retained in the sequential fractionation of flagella into axonemes and ribbons (Figure 3B). These cross-reactions provide convincing evidence that our cDNA clones pBrib43a and pBrib43aΔN64 contain the coding regions for the full-length and truncated forms of rib43a, respectively. We will now refer to wild-type protein and the protein cloned from *C. reinhardtii* ribbons as rib43a.

Sequence Analysis of Rib43a

By sequence analysis, rib43a does not possess primary sequence homology to any complete amino acid or nucleic acid sequences presently in the databanks, including those of tektins (i.e., only 10% identity and 23% similarity to tektins). However, rib43a does have a high degree of identity and similarity with partial clones from the flagellate *Trypanosoma cruzi* and human tumor cells from *Homo sapiens* (Figure 4) Comparing the predicted amino acid sequence of rib43a with that of the trypanosome expressed sequence tag

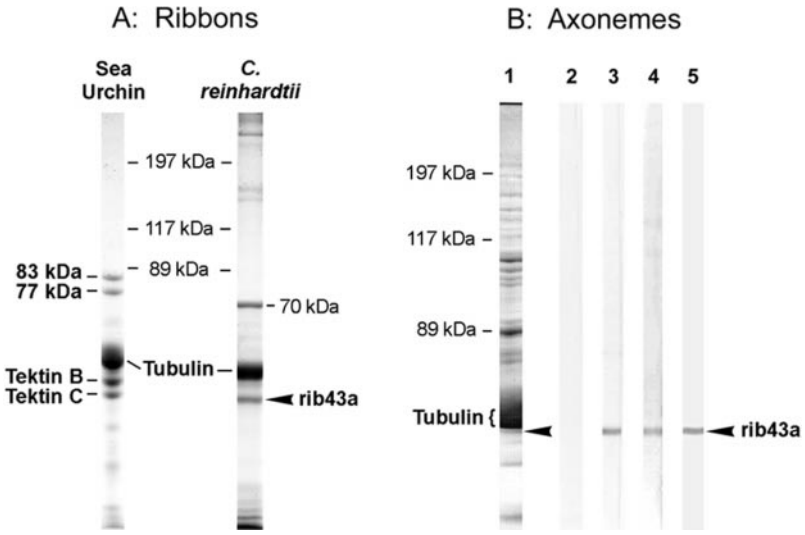

Figure 1. SDS-PAGE of ribbons and Western blot analysis with anti-rib43a antibodies. (A) Sarkosyl-insoluble ribbons (20 μg/lane) from sea urchin *Strongylocentrotus purpuratus* sperm flagella and *C. reinhardtii* flagella, showing tubulin and the main components of *S. purpuratus* (tektin-B ≅ 51-kDa, tektin-C ≅ 47-, 77-, and 83-kDa polypeptides; tektin-A ≅ 53-kDa comigrates with tubulin) and of *C. reinhardtii*. Calibration masses are given at 89, 117, and 197 kDa. The *C. reinhardtii* protein rib43a was isolated, transferred to nitrocellulose, and used to raise polyclonal rabbit antibodies for subsequent cloning. (B) SDS-PAGE blots of *Chlamydomonas* axonemes (40 μg/lane) demonstrating the specificity of anti-rib43a antibodies. Lane 1, protein stain; lane 2, preimmune sera; lane 3, whole anti-rib43a antisera; lane 4, affinity-purified anti-rib43a antibodies; lane 5, affinity-purified anti-rib43aΔN64 antibodies (against the expression protein; see text). Calibration masses are given in kilodaltons; arrowheads indicate the position of the rib43a protein, with a nominal molecular weight of 46,000.

(EST), the identity/similarity values are 35/47%; comparing rib43a with the human tumor ESTs, these values are 28/37% for EST1 (endometrial adenocarcinomas) and 26/38% for EST2 (germ cell tumors). The last search before publication revealed additional potential human rib43a homologues, including 1) a partial cDNA from fetal kidney (GenBank accession number AL050075) containing an open reading frame coding for a 150-residue polypeptide with an identity/similarity to rib43a of 27/54%, 2) a genomic sequence from chromosome 22 (GenBank accession number AL021391) with two regions, whose predicted polypeptides show identities/similarities to rib43a of 37/54% and 34/57%, and 3) a genomic sequence from chromosome X (GenBank accession number Z97054) with two regions, whose predicted polypeptides show identities/similarities to rib43a of 34/50% and 30/51%. Several blocks of amino acid residues are identically conserved between rib43a and the trypanosome EST (e.g., RVGDDD) and between rib43a and the human sequences AI890123, AI671905, AL050075, AL021391, and Z97054 (e.g., KGMT).

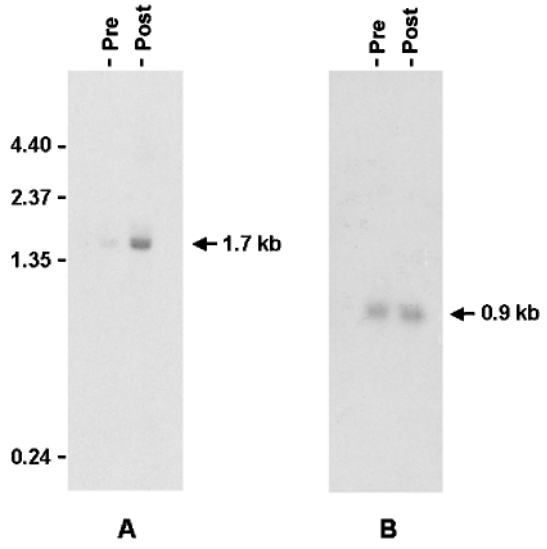

Figure 2. Northern blots of poly(A)$^+$ RNA (5 μg/lane) isolated from *Chlamydomonas* before and after (30 min) deflagellation. (A) pBrib43a hybridizes with a 1.7-kb band, which is up-regulated after deflagellation. (B) pCRY1-1, a clone coding for the S14 ribosomal protein, which is not involved in flagellar assembly (Nelson *et al.*, 1994), hybridizes with 0.9-kb bands of equal intensity before and after deflagellation. These results demonstrate that the up-regulation seen with pBrib43a is not due to unequal loading of RNA.

By analysis of secondary and tertiary structure, rib43a has an ~150-residue N-terminal sequence of undefined structure, followed by ~200 residues predicted to form several major segments of α-helix capable of forming coiled coils, separated by nonhelical linkers (Figure 5).

Isolation and Structure of the RIB43a Genomic Clone

We next isolated a *RIB43a* genomic clone to characterize the structure, sequence, and location of the gene on the genetic map of *Chlamydomonas* and to use it in the transformation of potential mutants. A λ genomic library, constructed from the wild-type strain *21gr* (Schnell and Lefebvre, 1993), was screened with the cDNA clone pBrib43aΔN64, and 11 overlapping clones were isolated. A 4634-bp fragment from one of these was subcloned into Bluescript to produce the genomic clone pRIB43a. The details of the gene are summarized in Figure 6.

Sequence analysis of the pRIB43a genomic clone identified the coding region contained within six exons. Within the coding region, a single-base pair difference was found between the sequences of the cDNA clone pBrib43a and the genomic clone pRIB43a. Nucleotide 493 of the cDNA sequence was determined to be a T in clone pBrib43a; the corresponding residue was ascertained to be a G in pRIB43a. This discrepancy may reflect a sequence variation in the *RIB43a* gene between the different strains used to construct the two libraries, i.e., *1132D−* for the cDNA library and *21gr* for the genomic library. Alternatively, the difference may

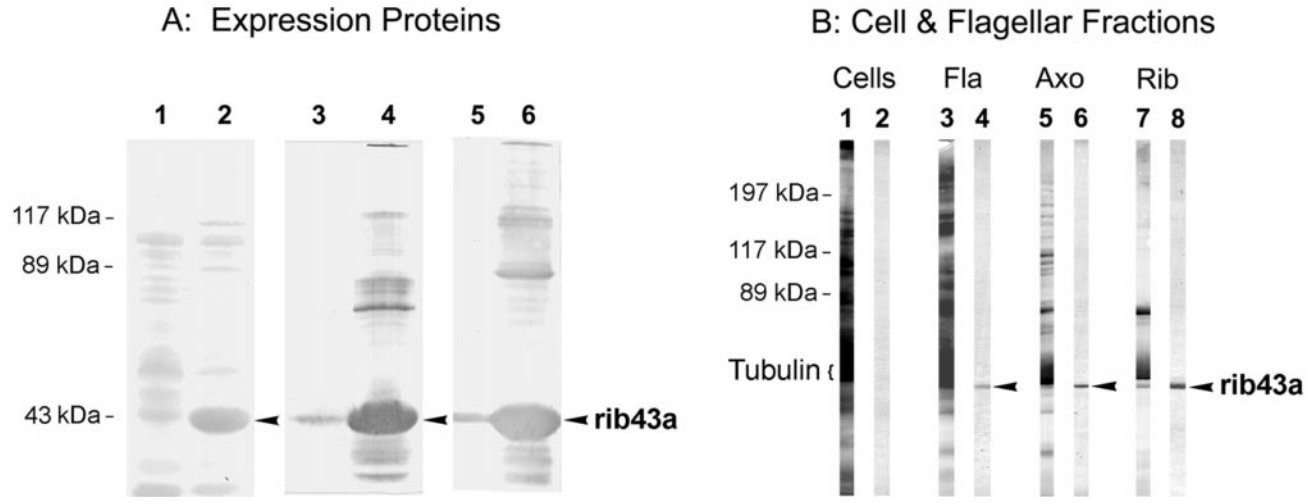

Figure 3. Western blot analysis of antibodies raised against the native *Chlamydomonas* ribbon protein rib43a (anti-rib43a) and against the bacterially expressed, truncated fusion protein from pBrib43aΔN64 (anti-rib43aΔN64). (A) SDS-PAGE blots of lysates from bacteria transformed with pBrib43aΔN64, as follows: lanes 1, 3, and 5, uninduced; lanes 2, 4, and 6, induced with IPTG. Lanes 1 and 2 were stained with Ponceau S; lanes 3 and 4 were stained with anti-rib43aΔN64; and lanes 5 and 6 were stained with anti-rib43a. The IPTG-induced fusion protein rib43aΔN64 (arrowheads) is recognized both by the antibody made against it (anti-rib43aΔN64, lane 4) and by anti-rib43a (lanes 6). (B) SDS-PAGE blots of whole *Chlamydomonas* cells (Cells, ~80 μg) and the sequential fractionation of flagella (Fla, 60 μg) into axonemes (Axo, 40 μg) and ribbons (Rib, 20 μg). Lanes 1, 3, 5, and 7, stained with Ponceau S; lanes 2, 4, 6, and 8, stained with affinity-purified anti-rib43aΔN64 antibodies (against the bacterially expressed fusion protein). Anti-rib43aΔN64 antibodies continue to stain the rib43a protein (arrowheads) that is retained in the purified ribbons after fractionation of flagella and axonemes. Only faint staining of rib43a could be seen in the original, freshly stained blot of whole cells; the apparent bands seen here are attributable to faint, uneven background across the nitrocellulose sheet.

represent an error in the reverse transcriptase reaction when the cDNA library was constructed.

Determination of Gene Copy and Mapping of the RIB43a Gene

To determine the copy number of the *RIB43a* gene, *Chlamydomonas* genomic DNA was analyzed by Southern blotting, probing with pRIB43a. The hybridization patterns indicate the presence of only one copy of *RIB43a* (Figure 7).

To determine the location of the *RIB43a* gene on the genetic map of *Chlamydomonas*, we used pRIB43a as a molecular marker to identify a restriction fragment length polymorphism between polymorphic strains of *C. reinhardtii*. The cosegregation of this restriction fragment length polymorphism was then analyzed with respect to 47 other genetic and molecular markers. *RIB43a* was found to map to linkage group III (our unpublished results) and is located between the radial spoke mutant *pf5* (Huang *et al.*, 1981) and the molecular marker Ef12e (Ranum *et al.*, 1988; Silflow *et al.*, 1995), which is linked to the flagellar assembly mutant *bld2* (Goodenough and St. Clair, 1975; Ehler *et al.*, 1995).

Efforts to Identify Function of RIB43a in Flagellar Mutants

To determine whether the *RIB43a* gene might be related to any of the flagellar mutations previously identified on linkage group III, we introduced wild-type copies of the *RIB43a* gene into both *bld2* and *pf5* mutant strains by cotransformation and screened for rescue of their respective motility defects. Analysis of >1000 cotransformants (with an expected cotransformation efficiency of 20%) indicated that *RIB43a* failed to rescue the mutant phenotypes. To confirm these results, we also isolated the *RIB43a* gene from these strains by PCR and sequenced through this region. The *RIB43a* gene was found to be wild type in both *bld2* and *pf5*.

EM of Ribbons and Localization of Rib43a

Ribbon preparations were assessed for purity, and their structure was examined by negative-stain EM. The ribbons were homogeneous in appearance, consisting of three adjoining protofilaments (Figure 8, A and B), and were indistinguishable at this resolution from the preparations originally reported by Witman *et al.* (1972) and from ribbons isolated from sea urchin sperm flagella (Nojima *et al.*, 1995). The ribbon preparations are rarely contaminated by structures other than an occasional singlet A-microtubule, one of which can be seen breaking down into a ribbon in Figure 8A. Some ribbons appear rigidly straight, others twisted and curled, and occasionally they lie side by side, forming sheets; these appearances are also similar to sea urchin ribbons (cf. Linck, 1990).

The rib43a protein was localized by indirect immuno-EM (Figure 8) and quantitated (Table 1), using as the primary antibodies affinity-purified anti-rib43a and affinity-purified anti-rib43aΔN64 and secondary 5-nm colloidal gold-conjugated goat anti-rabbit IgG. The antibodies labeled the ribbons with high specificity, but sparsely and randomly along their lengths and at their ends (Figure 8, C–E). The appearance of the antibody-treated ribbons (Figure 8, C–E) differs

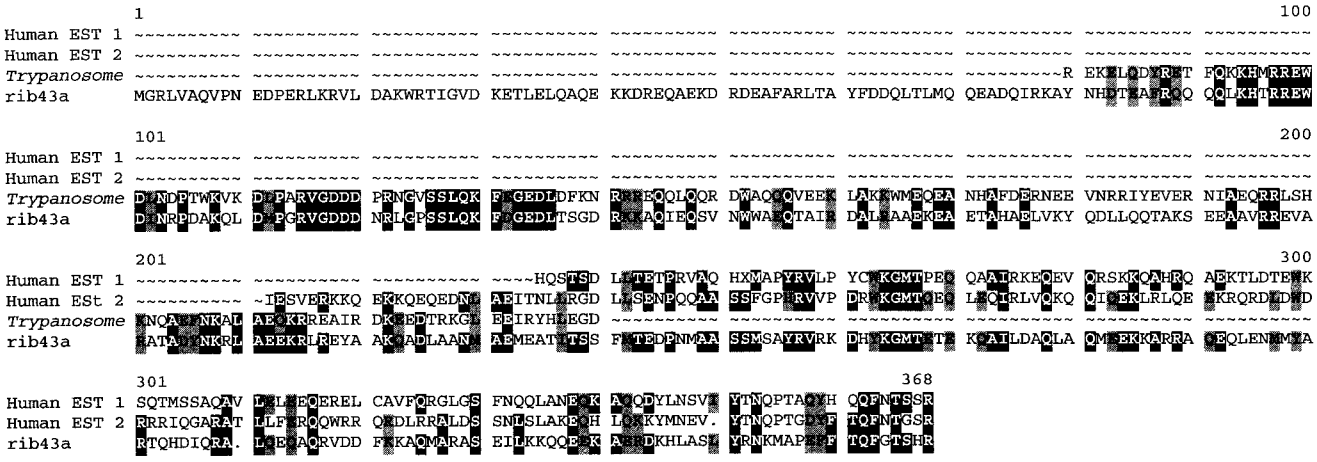

Figure 4. Predicted sequence of rib43a and comparison with other sequences in the database. The largest open reading frame of the pBrib43a cDNA consists of 1612 bp encoding rib43a, the 367-amino-acid protein from *Chlamydomonas* ribbons with a molecular weight of 42,638. The predicted sequence of rib43a is compared with sequences (ESTs) from *T. cruzi* and tumors of *H. sapiens*. Compared with rib43a, identical and conservatively substituted residues are shown in black and gray, respectively. Between rib43a and the *Trypanosoma* EST there is 35% identity and 46% similarity (similarity = identities + conservative substitutions) with no gaps in the sequences; between rib43a and the human tumor ESTs these values are 28 and 37% for EST1 and 26 and 38% for EST2 (with only one gap). Several blocks of amino acid residues are identically conserved between rib43a and the trypanosome EST (e.g., RVGDDD) and between rib43a and both of the human tumor ESTs (e.g., KGMT). Note that rib43a has no cysteine residues. The references of the clones are as follows: rib43a (this report; GenBank accession numbers AF196576 for the cDNA clone and AF196577 for the genomic clone); *Trypanosome* (GenBank accession number AI080816); human EST1 (GenBank accession number AI890123) from moderately differentiated, endometrial adenocarcinoma, three pooled tumors; and human EST2 (GenBank accession number AI671905) from pooled germ cell tumors.

significantly from the starting preparation (Figure 8, A and B) and from sea urchin ribbons. This difference may arise both from the obscuring of the structure by the blocking proteins and antibodies and from the possible breakdown of the ribbons during the prolonged incubations (sea urchin ribbons are more stabile to these treatments; Amos *et al.*, 1986). Nevertheless, the three-protofilament substructure of this immunostained material is occasionally apparent (Figure 8E). Some labeled particles initially appeared to be nonspecific background, but at higher magnification the gold label was clearly associated with thin fibrils (<5 nm in diameter) of heterogeneous lengths (>100 nm; Figure 8E). No labeling was seen on the ribbons, on the short fibrils, or on the grid film support, if blocking buffer (Figure 8F) or preimmune sera (our unpublished results) were used in place of the specific antibody, nor did gold-conjugated antibody adhere to the grid film in the absence of ribbon sample. These observations were supported by quantitative analysis.

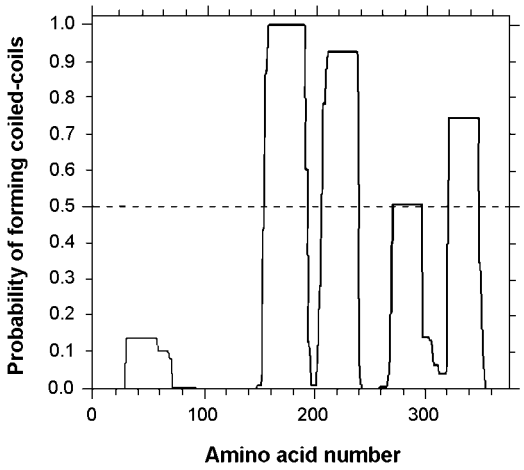

Figure 5. Predicted coiled-coil structure of *Chlamydomonas* rib43a, using the CoilScan program (Lupas *et al.*, 1991; Lupas, 1996). Probability of the formation of coiled coil (ordinate) is plotted along the polypeptide chain from N to C terminus (abscissa).

The quantitation of the gold particles is shown in Table 1, based on images similar to and including Figure 8 (see MATERIALS AND METHODS). Gold particle counts were extremely low in the controls, i.e.: 1) no sample (blocking protein only), followed by primary antibody (affinity-purified anti-rib43aΔN64 antibodies), followed by 1:50 dilution of secondary antibody; 2) no sample, zero primary antibody, 1:50 secondary antibody; and 3) ribbon sample, zero primary antibody, 1:50 secondary antibody. In the experimental samples treated with lower concentrations of secondary antibody (1:200 dilution), the number of gold particles observed increased dramatically. At primary antibody dilutions of 1:500, the number of particles considered bound (<23 nm from ribbons and fibrils) was 130 (normalized to the area observed). At a higher concentration of primary antibody (1:200 dilution) the number of bound particles increased to 548 (4.2 times), whereas the increases in the numbers of apparently unbound or unassigned particles were significantly less (1.3 and 1.5 times, respectively). The counts of

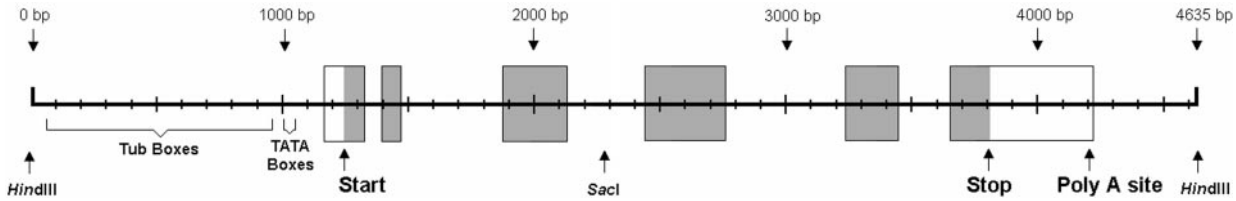

Figure 6. The structure of the 4.4-kb wild-type genomic fragment containing the *RIB43a* gene. Boxed areas indicate sequence contained in the cDNA clone pBrib43a; shaded boxes designate the largest open reading frame. Comparison of the cDNA length (1612 bp) with the estimated size of the *RIB43a* transcript (~1700 bases by Northern blotting; Figure 2) puts the transcription initiation site at ~1051 bases; the predicted translation start codon is located at base 1244. There are 11 potential tub boxes (at least 70% identical to the consensus sequence GTTCSAAGGC; Davies and Grossman, 1994) located at bases 48, 136, 318, 397, 425, 535, 542, 694, 783, 879, and 953; these sequence elements are thought to be important for regulated expression of flagellar transcripts. Potential TATA boxes are located at 1007 bases (TTTATGA), 1009 bases (TATGATA), 1012 bases (GATAATT), and 1046 bases (TACACAT). The translation stop codon is present at base 3808. A polyadenylation site (TGTAA) appears at base 4202; the start of the poly(A) tail on our cDNA corresponds to base 4220 of the genomic sequence.

ribbons versus fibrils could not be quantitated, because it was not always possible to distinguish among ribbons, frayed ribbons, ribbons lying on their edges, and groups of fibrils; nevertheless, examples of all of these structures were seen to be labeled (Figure 8E). The correlation between the increase in bound gold particles and the higher concentration of primary antibody paralleled a feature that was qualitatively observed by EM; i.e., as the concentration of primary antibody was increased (from 1:500 to 1:200 dilutions), the amount of fraying of the ribbons and the amount of fibrils appearing also increased significantly. Finally, a higher than random labeling of the ends of ribbons and fibrils was observed, i.e., 27% at a primary antibody dilution of 1:500; at a 1:200 dilution there was too much fraying and too many fibrils to accurately determine end counts.

As is known from previous studies, sea urchin ribbons can be extracted with 2 M urea to solubilize the associated tubulin and other proteins, leaving intact, 2- to 5-nm-diam filaments composed of tektins A, B, and C (Pirner and Linck, 1994). We applied this method in the hope of fractionating the ribbons of *Chlamydomonas* into filaments of rib43a, but these treatments dissolved the ribbons completely; i.e., residual filaments were not observed by EM or recovered by ultracentrifugation.

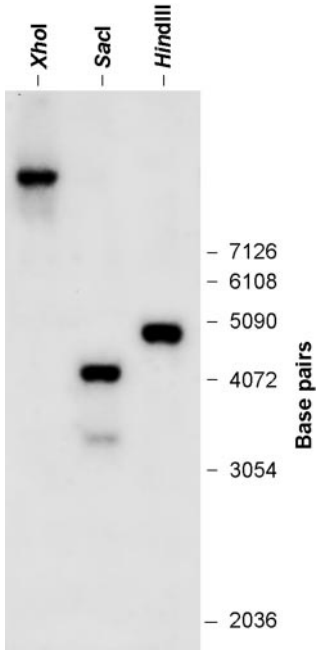

Figure 7. Southern blot analysis of gene copy number. The hydridization pattern of blots of genomic DNA digested with *Xho*I, *Sac*I, and *Hin*dIII probed with pBrib43a agrees with the restriction patterns predicted from the pRIB43a sequence. This suggests there is a single *RIB43a* gene. Size standards are indicated on the right.

Immunofluorescence Localization of Rib43a

By immunofluorescence microscopy, affinity-purified anti-rib43aΔN64 antibodies stained the flagella in a punctate pattern from base to tip. The most intensely stained region was the intracellular bases of the flagella (Figure 9). When preimmune sera (Figure 9, E and F) was used, or when no rabbit antibody (i.e., blocking buffer; our unpublished observations) was applied, neither the flagella nor the basal region stained, and there was only a diffuse, nonspecific staining of the cell body. This nonspecific background is consistent with other reports on *Chlamydomonas* (Cole *et al.*, 1998); furthermore, we observe a lack of cross-reaction of anti-rib43aΔN64 antibodies with antigens on immunoblots of whole cells (Figure 3B, lanes 1 and 2). To eliminate the background fluorescence caused by the chloroplast and other cellular constituents, we isolated flagellar-basal body apparatuses by the technique of Wright *et al.* (1985) or by detergent extraction of cells attached to coverslips. Under these conditions the staining was more intense, and the background was reduced substantially. The flagella stained in the same punctate manner as before, from base to tip, but the staining at their base was significantly brighter relative to background. In numerous cases, the basal region of staining could be resolved into two spots, corresponding in position to the basal bodies. We conclude, therefore, that the rib43a-specific antibodies identify rib43a and/or homologous proteins in both flagella and basal bodies. In addition, the anti-rib43a antibodies were observed to stain structures corresponding to the proximal portion of the four rootlet microtubules.

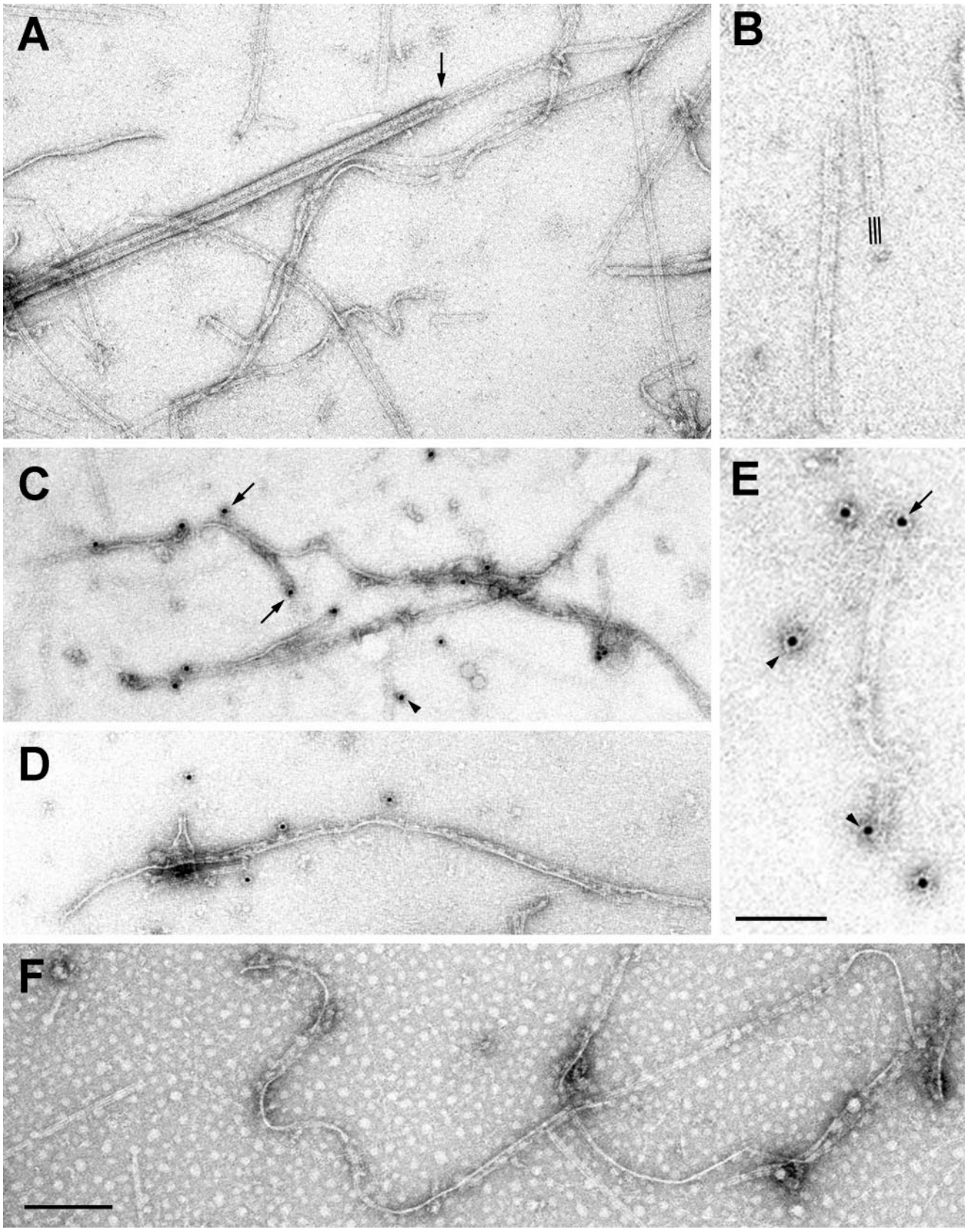

Figure 8.

Table 1. Quantitation of immuno-EM labeling

Preparation	No. of particles <23 nm from ribbon/fibril[a]	% of particles <23 nm from end of ribbon/fibril	No. of particles >23 nm from ribbon/fibril[c]	Unassigned particles[d]
Area examined	**Normalized[b]**		**Normalized**	**Normalized**
Control: no sample				
1:200 primary Ab[e]	0	0	7 (in 1 cluster)	0
1:50 secondary Ab[f]	**0**		**11**	**0**
65 μm^2				
Control: no sample				
0 primary Ab	0	0	0	0
1:50 secondary Ab	**0**		**0**	**0**
65 μm^2				
Control: sample				
0 primary Ab	1	X[g]	0	0
1:50 secondary Ab	**1**		**0**	**0**
113 μm^2				
Sample				
1:500 primary Ab	147	27	146	39
1:200 secondary Ab	**130**		**129**	**35**
113 μm^2				
Sample				
1:200 primary Ab	411	ND	138	40
1:200 secondary Ab	**548**		**184**	**53**
75 μm^2				

Total particles counted: 921.

[a] The measure of specific antibody binding to ribbons and fibrils.

[b] Normalized values = number of particles/$\mu m^2 \times 100$.

[c] Maximum estimate of nonlabeling; however, particles may be labeling single, unresolved protein subunits.

[d] Includes particles positioned near edge of field or over unrecognizable material.

[e] Primary, affinity-purified, rabbit anti-rib43aΔN64 antibodies.

[f] Secondary, 5-nm gold-conjugated, goat anti-rabbit IgG. Note that a higher concentration was used on controls than on experimental samples.

[g] The only particle observed was at the end of a ribbon.

DISCUSSION

Flagellar microtubules of *Chlamydomonas* and echinoderm sperm are similar in that they can be fractionated into stable ribbons of three adjoining protofilaments by Sarkosyl extraction (Figure 8A; Meza *et al.*, 1972; Witman *et al.*, 1972a,b; Linck, 1990). Echinoderm ribbons have been characterized more extensively and are composed of α- and β-tubulin, 83- and 77-kDa polypeptides, at least three tektins (A, ≅53 kDa; B, ≅51 kDa; and C, ≅47 kDa), and several polypeptides ≤38 kDa (Linck, 1990; Hinchcliffe and Linck, 1998). Heat-stable, tektin-containing protofilament remnants have also been isolated from molluscan cilia (Stephens *et al.*, 1989) and ctenophore cilia (Linck *et al.*, 1991); interestingly, the architectural remnants of molluscan gill ciliary A-microtubules remain connected in a ninefold axonemal pattern by nexin links (Stephens *et al.*, 1989). The cloned sequences of sea urchin tektins (Norrander *et al.*, 1992, 1996; Chen *et al.*, 1993) and the tektin C homologue from mouse testis (Norrander *et al.*, 1998) have been rigorously analyzed, and structural studies have shown tektins to form a continuous, longitudinal filament of the A-tubule (Nojima *et al.*, 1995). Tektins and tektin filaments have observed and predicted axial spacings that match with those of dynein arms, radial spokes, and nexin links, suggesting that tektins have molecular ruler properties (Nojima *et al.*, 1995; Pirner and Linck, 1994; Norrander *et al.*, 1996). *Chlamydomonas* ribbons have a somewhat different polypeptide composition, i.e., α- and β-tubulin, two major protein bands of ~72 and ~46 kDa, and several other polypeptides in lesser amounts (Figure 1). We have

Figure 8 (facing page). Negative stain and immuno-EM of *Chlamydomonas* ribbons. (A and B) Preparation of purified ribbons, negatively stained with 1% uranyl acetate. Ribbons are homogeneously composed of three protofilaments (three lines in B). Some ribbons are straight and rigid, and others are twisted and curled; some ribbons form pairs or sheets. A rare, contaminating A-microtubule is included for size comparison and to show the ribbon emerging from its end (arrow). (C–E) Ribbons stained with affinity-purified, rabbit anti-rib43aΔN64 antibodies, followed by 5-nm colloidal gold-conjugated goat anti-rabbit IgG. Ribbons are sparsely and randomly labeled along their length and at their ends (arrows). Many apparent background gold particles are actually due to label on short pieces of ribbons and on short, thin fibrils (arrowheads). (F) Control showing absence of staining when primary antibody is omitted. Bars, A, C, D, and F, 0.2 μm; B and E, 100 nm.

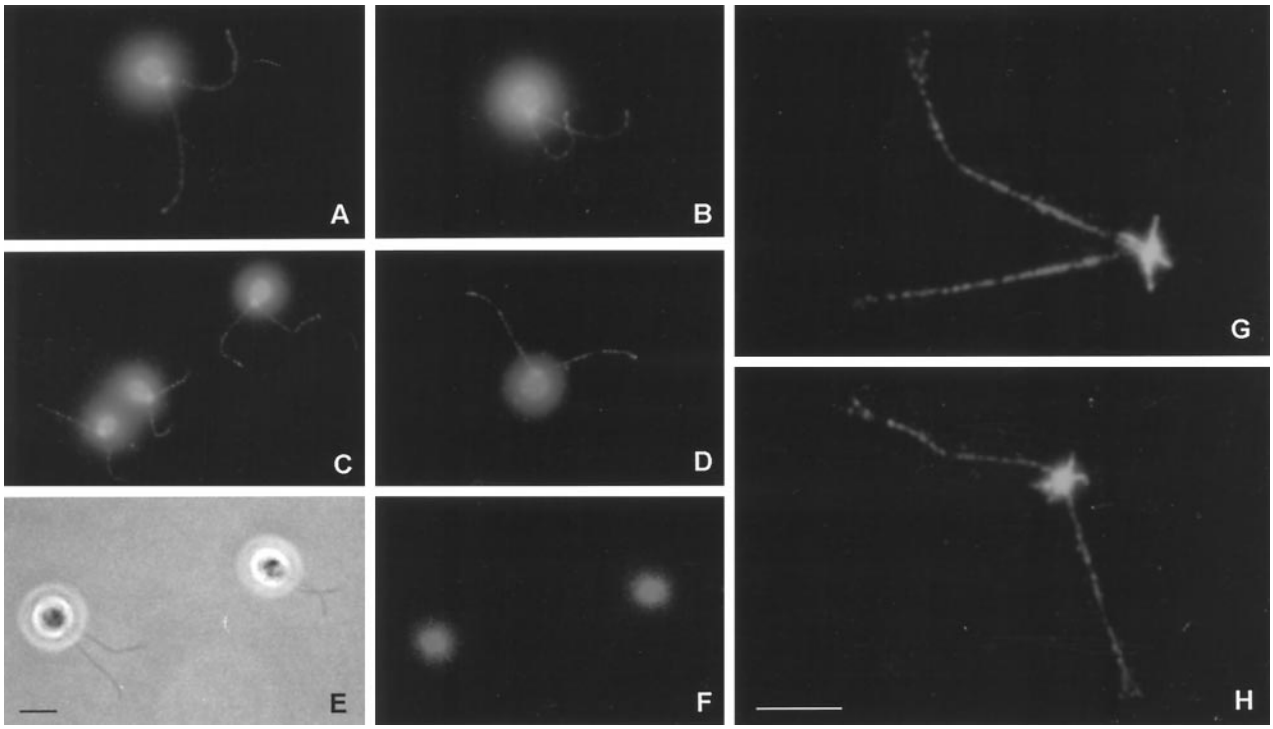

Figure 9. Immunofluorescence microscopy of whole cells and basal body–flagellar complexes. (A–D) Cells stained with affinity-purified rabbit anti-rib43aΔN64 antibody, followed by Texas Red-conjugated goat anti-rabbit IgG. (E) Phase-contrast image; (F) lack of staining with preimmune serum. (G and H) Immunofluorescence of isolated basal body–flagellar apparatuses stained with anti-rib43aΔN64. These results demonstrate that anti-rib43a antibodies specifically stain basal bodies and flagella in a punctate manner from base to tip. In addition, the anti-rib43a antibodies stained structures corresponding to the proximal portion of the four rootlet microtubules (G and H). Bars, A–F, 5 μm; G and H, 5 μm.

concentrated in this report on the characterization of the ~46-kDa polypeptide, rib43a, which by sequencing has a calculated mass of ≅43 kDa.

Our results demonstrate that the rib43a protein is associated with forming the specialized protofilament ribbons of flagellar microtubules in *Chlamydomonas*. The RIB43a gene has canonical features of a flagellar gene (Figure 6) and is up-regulated after flagellar amputation (Figure 2). Antibodies against its cloned, expressed form, rib43aNΔ64, demonstrate by Western blots that rib43a is retained in ribbons after flagellar fractionation (Figure 3B), and anti-rib43aNΔ64 antibodies label isolated ribbons by immuno-EM (Figure 8).

Rib43a is an integral component of ribbons, although its exact structure within ribbons is unknown. Anti-rib43aNΔ64 antibodies specifically label ribbons (Figure 8 and Table 1), although the labeling is sparse and random along their length, with a significantly higher degree of labeling (27%) at their ends. This pattern resembles that of anti-tektin labeling of sea urchin ribbons. Anti-tektin labeling occurs only at the ends of sea urchin ribbons (where tektin filaments protrude) and not along their length, unless the tubulin protofilaments are solubilized to expose the underlying, insoluble tektin filaments (Linck *et al.*, 1985; Amos *et al.*, 1986). Such a labeling pattern is not the case with Sp83, the 83-kDa polypeptide of sea urchin ribbons, along which anti-Sp83 antibodies readily label (Hinchcliffe and Linck, 1998). These results suggest a model in which rib43a, like tektin, is assembled into the ribbon with its antigenic sites inaccessible (e.g., due to its conformation and/or to masking by tubulin). This model would also explain the punctate, immunofluorescence patterns of *Chlamydomonas* axonemes stained with anti-rib43a (Figure 9) and sea urchin axonemes stained with anti-tektins (Linck *et al.*, 1987).

The treatment of *Chlamydomonas* ribbons with a 2.5 higher concentration of anti- rib43aNΔ64 antibodies has two affects on their structure. First, there is a quantitative, 4.2 times increase in the degree of labeling along the ribbons (Table 1). Second, there is a qualitative structural change. At the higher antibody concentration ribbons appear more frayed, and there is an increase in the number of long and short fibrils that also label with the antibody (Figure 8E); however, the ribbons, frayed ribbons, and bundles of fibrils could not easily be distinguished for quantitation. These results raise the possibility that antibody binding to rib43a causes a dissociation of the ribbons. (By contrast, sea urchin ribbons do not disintegrate when treated with anti-tektin antibodies [Amos *et al.*, 1986].) The antibody labeling of the fibrils suggests that the fibrils are composed partly or entirely of rib43a. The coiled-coil structure of rib43a (Figure 5) is consistent with such a fibrous structure; however, it has not yet been possible to isolate stable, extended polymers of rib43a, as is possible with sea urchin tektins. Rib43a contains no cysteine residues, whereas tektins typically contain four cysteines, one in each of four nonhelical linkers (Norrander *et*

al., 1998). Preliminary cross-linking studies suggest that disulfide bonds in tektins may act to stabilize the tektin AB heterodimeric polymer (Pirner and Linck, 1994, 1995; Moran and Linck, unpublished results). Potentially, the lack of cysteines in rib43a could account for its dissociation by Sarkosyl-urea solvents and anti-rib43aNΔ64 antibodies. The potential for rapid dissociation might be biologically important in the resorption of flagella during the cell cycle of *Chlamydomonas* (Cavalier-Smith, 1974); in contrast, sperm flagella of higher organisms are well known to be irreversibly assembled (Baccetti and Afzelius, 1976). Given our *RIB43a* clone and its probes, these models are now testable biochemically and genetically.

The immunofluorescence staining of *Chlamydomonas* (Figure 9) indicates that certain ribbon proteins are also integral components of basal bodies, consistent with observations with other species. Affinity-purified, polyclonal antibodies raised against individually purified echinoderm tektins A, B, and C and against ribbon components Sp77 and Sp83, stain echinoderm sperm basal bodies more intensely than the associated flagellar axonemes; furthermore, many of these antibodies stain centrioles in a variety of mammalian cells, including *H. sapiens* (Steffen and Linck, 1988, 1989; Hinchcliffe and Linck, 1998). Quantitative studies of molluscan gill epithelia have shown that basal bodies contain approximately twice the amount of tektins per unit length of microtubule, compared with ciliary axonemes (Stephens and Lemieux, 1998). These results support the model in which centriole and basal body A-tubules contain specialized protofilament ribbons that are similar to those extending into the A-tubules of doublet microtubules. However, to date, the only basal body-specific gene to be cloned, *UNI3*, encodes δ-tubulin (Dutcher and Trabuco, 1998), which is required for forming basal body C-tubules.

Finally, rib43a bears no primary sequence homology to tektins from sea urchin or to tektin homologues from evolutionarily earlier organisms, i.e., *C. elegans* or *Drosophila* (Norrander *et al.*, 1998). The fact that none of our sea urchin tektin antibodies or cDNAs cross-react or hybridize with *Chlamydomonas* may indicate either that *Chlamydomonas* has no tektin equivalents or that it has functionally equivalent proteins, including perhaps rib43a. Whatever the case, we have identified a novel gene encoding a protein that 1) is structurally integral to *Chlamydomonas* flagellar protofilament ribbons and 2) is homologous to sequences from trypanosomes and human cells (Figure 4). The presence of a trypanosome rib43a homologue is not surprising in a flagellated protozoan parasite, whereas human rib43a homologues could represent a structural requirement in centriole replication in dividing cells. These all remain testable speculations.

ACKNOWLEDGMENTS

We thank Drs. Curtis Wilkerson and George Witman for the λZapII expression library, Dr. Ryoko Kuriyama for use of her Olympus microscope, Dr. Catherine Perrone for helpful technical assistance and advice, and Drs. Pete Lefebvre and Carolyn Silflow and members of their laboratories for constructive criticism and scientific advice. Finally, we are pleased to thank Monitoring Editor J. Richard McIntosh and the reviewers for a most constructive dialogue. This work was supported by US Public Health Service grant GM-35648 and University of Minnesota Graduate School grant 17936 (to R.W.L.), US Public Health Service grant GM-55667 and National Science Foundation grant MCB-9305217 (to M.E.P.), and National Science Foundation Research Training Group grants BIR-9113444 and DBI-9602237.

REFERENCES

Afzelius, B.A. (1995). Situs inversus and ciliary abnormalities. What is the connection? Int. J. Dev. Biol. *39*, 839–844.

Allen, C., and Borisy, G.G. (1974). Structural polarity and directional growth of microtubules of *Chlamydomonas* flagella. J. Mol. Biol. *90*, 381–402.

Altschul, S.F., Gish, W., Miller, W., Myers, E.W., and Lipman, D.J. (1990). Basic local alignment search tool. J. Mol. Biol. *215*, 403–410.

Amos, W.B., Amos, L.A., and Linck, R.W. (1986). Studies of tektin filaments from flagellar microtubules by immunoelectron microscopy. J. Cell. Sci. Suppl. *5*, 55–68.

Amos, L., and Klug, A. (1974). Arrangement of subunits in flagellar microtubules. J. Cell Sci. *14*, 523–549.

Aviv, H., and Leder, P. (1972). Purification of biologically active globin mRNA by chromatography on oligothymidylic acid-cellulose. Proc. Natl. Acad. Sci. USA *69*, 1408–1412.

Baccetti, B., and Afzelius, B.A. (1976). The biology of the sperm cell. In: Monographs in Developmental Biology, vol. 10, ed. A. Wolsky, Basel: S. Karger, 254.

Cavalier-Smith, T. (1974). Basal body and flagellar development during the vegetative cell cycle and the sexual cycle of *Chlamydomonas reinhardii*. J. Cell Sci. *16*, 529–556.

Chen, J., Knowles, H.J., Hebert, J.L., and Hackett, B.P. (1998). Mutation of the mouse hepatocyte nuclear factor/forkhead homologue 4 gene results in an absence of cilia and random left-right asymmetry. J. Clin. Invest. *102*, 1077–1082.

Chen, R., Perrone, C.A., Amos, L.A., and Linck, R.W. (1993). Tektin B1 from ciliary microtubules: primary structure as deduced from the cDNA sequence and comparison with tektin A1. J. Cell Sci. *106*, 909–918.

Cole, D.G., Diener, D.R., Himelblau, A.L., Beeche, P.L., Fuster, J.C., and Rosenbaum, J.L. (1998). *Chlamydomonas* kinesin-II-dependent intraflagellar transport (IFT): IFT particles contain proteins required for ciliary assembly in *Caenorhabditis elegans* sensory neurons. J. Cell Biol. *141*, 993–1008.

Collet, J., Spike, C.A., Lundquist, E.A., Shaw, J.E., and Herman, R.K. (1998). Analysis of osm-6, a gene that affects sensory cilium structure and sensory neuron function in *Caenorhabditis elegans*. Genetics *148*, 187–200.

Davies, J.P., and Grossman, A.R. (1994). Sequences controlling transcription of the *Chlamydomonas reinhardtii* beta 2-tubulin gene after deflagellation and during the cell cycle. Mol. Cell. Biol. *14*, 5165–5174.

Dutcher, S.K. (1986). Genetic properties of linkage group XIX in *Chlamydomonas reinhardtii*. In: Extrachromosomal Elements in Lower Eukaryotes, ed. R.B. Wickner, A. Hinnebusch, A.M. Lambowitx, I.D. Gunsalaus, and A. Hollaender, New York: Plenum Press, 303–325.

Dutcher, S.K. (1995). Flagellar assembly in two hundred and fifty easy-to-follow steps. Trends Genet, *11*, 398–404.

Dutcher, S.K., and Trabuco, E.C. (1998). The UNI3 gene is required for assembly of basal bodies of *Chlamydomonas* and encodes delta-tubulin, a new member of the tubulin superfamily. Mol. Biol. Cell *9*, 1293–1308.

Ehler, L.L., Holmes, J.A., and Dutcher, S.K. (1995). Loss of spatial control of the mitotic spindle apparatus in a *Chlamydomonas reinhardtii* mutant strain lacking basal bodies. Genetics *141*, 945–960.

Fowkes, M.E., and Mitchell, D.R. (1998). The role of preassembled cytoplasmic complexes in assembly of flagellar dynein subunits. Mol. Biol. Cell *9*, 2337–2347.

Gardner, L.C., O'Toole, E., Perrone, C.A., Giddings, T., and Porter, M.E. (1994). Components of a "dynein regulatory complex" are located at the junction between the radial spokes and the dynein arms in *Chlamydomonas* flagella. J. Cell Biol. *127*, 1311–1325.

Gibbons, B.H., and Gibbons, I.R. (1979). Relationship between the latent adenosine triphosphatase state of dynein 1 and its ability to recombine functionally with KCl-extracted sea urchin sperm flagella. J. Biol. Chem. *254*, 197–201.

Gibbons, I.R. (1981). Cilia and flagella of eukaryotes. J. Cell Biol. *91*, 107s–124s.

Goodenough, U.W., and Heuser, J.E. (1985a). Outer and inner dynein arms of cilia and flagella. Cell *41*, 341–342.

Goodenough, U.W., and Heuser, J.E. (1985b). Substructure of inner dynein arms, radial spokes, and the central pair/projection complex of cilia and flagella. J. Cell Biol. *100*, 2008–2018.

Goodenough, U.W., and St.Clair, H.S. (1975). BALD-2: a mutation affecting the formation of doublet and triplet sets of microtubules in *Chlamydomonas reinhardtii*. J. Cell Biol. *66*, 480–491.

Haimo, L.T., Telzer, B.R., and Rosenbaum, J.L. (1979). Dynein binds to and cross-bridges cytoplasmic microtubules. Proc. Natl. Acad. Sci. USA *76*, 5759–5763.

Harris, E.H. (1989). The Chlamydomonas Sourcebook: A Comprehensive Guide to Biology and Laboratory Use, San Diego: Academic Press.

Hinchcliffe, E.H., and Linck, R.W. (1998). Two proteins isolated from sea urchin sperm flagella: structural components common to the stable microtubules of axonemes and centrioles. J. Cell Sci. *111*, 585–595.

Huang, B., Piperno, G., and Luck, D.J. (1979). Paralyzed flagella mutants of *Chlamydomonas reinhardtii*. Defective for axonemal doublet microtubule arms. J. Biol. Chem. *254*, 3091–3099.

Huang, B., Piperno, G., Ramanis, Z., and Luck, D.J. (1981). Radial spokes of *Chlamydomonas* flagella: genetic analysis of assembly and function. J. Cell Biol. *88*, 80–88.

James, S.W., Silflow, C.D., Stroom, P., and Lefebvre, P.A. (1993). A mutation in the alpha 1-tubulin gene of *Chlamydomonas reinhardtii* confers resistance to antimicrotubule herbicides. J. Cell Sci. *106*, 209–218.

Keil, T.A. (1997). Functional morphology of insect mechanoreceptors. Microsc. Res. Tech. *39*, 506–531.

King, S.M., Otter, T., and Witman, G.B. (1986). Purification and characterization of *Chlamydomonas* flagellar dyneins. Methods Enzymol. *134*, 291–306.

Laemmli, U.K. (1970). Cleavage of structural proteins during the assembly of the head of bacteriophage T4. Nature *227*, 680–685.

Lefebvre, P.A. (1995). Flagellar amputation and regeneration in *Chlamydomonas*. Methods Cell Biol. *47*, 3–7.

Linck, R.W. (1990). Tektins and microtubules. In: Advances in Cell Biology, ed. K.R. Miller, London: JAI Press, 35–63.

Linck, R.W., Amos, L.A., and Amos, W.B. (1985). Localization of tektin filaments in microtubules of sea urchin sperm flagella by immunoelectron microscopy. J. Cell Biol. *100*, 126–135.

Linck, R.W., Goggin, M.J., Norrander, J.M., and Steffen, W. (1987). Characterization of antibodies as probes for structural and biochemical studies of tektins from ciliary and flagellar microtubules. J. Cell Sci. *88*, 453–466.

Linck, R.W., Stephens, R.E., and Tamm, S.L. (1991). Evidence for tektins in cilia from the ctenophore, *Mnemiopsis leidyi*. In: Comparative Spermatology 20 Years After, Serono Symposia Publications vol. 75, ed. B. Baccetti, New York: Raven Press, 391–395.

Lupas, A. (1996). Prediction and analysis of coiled-coil structures. Methods Enzymol. *266*, 513–25.

Lupas, A., Van Dyke, M., and Stock, J. (1991). Predicting coiled coils from protein sequences. Science *252*, 1162–1164.

Mastronarde, D.N., O'Toole, E.T., McDonald, K.L., McIntosh, J.R., and Porter, M.E. (1992). Arrangement of inner dynein arms in wild-type and mutant flagella of *Chlamydomonas*. J. Cell Biol. *118*, 1145–1162.

Meza, I., Huang, B., and Bryan, J. (1972). Chemical heterogeneity of protofilaments forming the outer doublets from sea urchin flagella. Exp. Cell Res. *74*, 535–540.

Mochizuki, T., *et al*. (1998). Cloning of *inv*, a gene that controls left/right asymmetry and kidney development. Nature *395*, 177–181.

Myster, S.H., Knott, J.A., O'Toole, E.T., and Porter, M.E. (1997). The *Chlamydomonas* Dhc1 gene encodes a dynein heavy chain subunit required for assembly of the I1 inner arm complex. Mol. Biol. Cell *8*, 607–620.

Nelson, J.A., Savereide, P.B., and Lefebvre, P.A. (1994). The CRY1 gene in *Chlamydomonas reinhardtii*: structure and use as a dominant selectable marker for nuclear transformation. Mol. Cell. Biol. *14*, 4011–4019.

Nojima, D., Linck, R.W., and Egelman, E.H. (1995). At least one of the protofilaments in flagellar microtubules is not composed of tubulin. Curr. Biol. *5*, 158–167.

Nonaka, S., Tanaka, Y., Okada, Y., Takeda, S., Harada, A., Kanai, Y., Kido, M., and Hirokawa, N. (1998). Randomization of left-right asymmetry due to loss of nodal cilia generating leftward flow of extraembryonic fluid in mice lacking KIF3B motor protein. Cell *95*, 829–837.

Norrander, J.M., Amos, L.A., and Linck, R.W. (1992). Primary structure of tektin A1: comparison with intermediate-filament proteins and a model for its association with tubulin. Proc. Natl. Acad. Sci. USA *89*, 8567–8571.

Norrander, J., Kempe, T., and Messing, J. (1983). Construction of improved M13 vectors using oligodeoxynucleotide- directed mutagenesis. Gene *26*, 101–106.

Norrander, J., Larsson, M., Stσhl, S., H÷÷g, C., and Linck, R. (1998). Expression of ciliary tektins in brain and sensory development. J. Neurosci. *18*, 8912–8918.

Norrander, J.M., Linck, R.W., and Stephens, R.E. (1995). Transcriptional control of tektin A mRNA correlates with cilia development and length determination during sea urchin embryogenesis. Development *121*, 1615–1623.

Norrander, J.M., Perrone, C.A., Amos, L.A., and Linck, R.W. (1996). Structural comparison of tektins and evidence for their determination of complex spacings in flagellar microtubules. J. Mol. Biol. *257*, 385–397.

Perkins, L.A., Hedgecock, E.M., Thomson, J.N., and Culotti, J.G. (1986). Mutant sensory cilia in the nematode *Caenorhabditis elegans*. Dev. Biol. *117*, 456–487.

Piperno, G., Huang, B., and Luck, D.J. (1977). Two-dimensional analysis of flagellar proteins from wild-type and paralyzed mutants of *Chlamydomonas reinhardtii*. Proc. Natl. Acad. Sci. USA *74*, 1600–1604.

Piperno, G., Ramanis, Z., Smith, E.F., and Sale, W.S. (1990). Three distinct inner dynein arms in *Chlamydomonas* flagella: molecular composition and location in the axoneme. J. Cell Biol. *110*, 379–389.

Pirner, M.A., and Linck, R.W. (1994). Tektins are heterodimeric polymers in flagellar microtubules with axial periodicities matching the tubulin lattice. J. Biol. Chem. *269*, 31800–31806.

Pirner, M.A., and Linck, R.W. (1995). Methods for the isolation of tektins and Sarkosyl-insoluble protofilament ribbons. Methods Cell Biol. *47*, 373–380.

Porter, M.E. (1996). Axonemal dyneins: assembly, organization, and regulation. Curr. Opin. Cell Biol. *8*, 10–17.

Porter, M.E., Knott, J.A., Myster, S.H., and Farlow, S.J. (1996). The dynein gene family in *Chlamydomonas reinhardtii*. Genetics *144*, 569–585.

Ranum, L.P., Thompson, M.D., Schloss, J.A., Lefebvre, P.A., and Silflow, C.D. (1988). Mapping flagellar genes in *Chlamydomonas* using restriction fragment length polymorphisms. Genetics *120*, 109–122.

Sambrook J., Fritsch, E., and Maniatis, T. (1989). Molecular Cloning: A Laboratory Manual, Cold Spring Harbor, NY: Cold Spring Harbor Laboratory Press.

Schnell, R.A., and Lefebvre, P.A. (1993). Isolation of the *Chlamydomonas* regulatory gene NIT2 by transposon tagging. Genetics *134*, 737–747.

Silflow, C.D., Chisholm, R.L., Conner, T.W., and Ranum, L.P. (1985). The two alpha-tubulin genes of *Chlamydomonas reinhardi* code for slightly different proteins. Mol. Cell. Biol. *5*, 2389–2398.

Silflow, C.D., Kathir, P., and Lefebvre, P.A. (1995). Molecular mapping of genes for flagellar proteins in *Chlamydomonas*. Methods Cell Biol. *47*, 525–530.

Smith, E.F., and Sale, W.S. (1992). Structural and functional reconstitution of inner dynein arms in *Chlamydomonas* flagellar axonemes. J. Cell Biol. *117*, 573–581.

Southern, E.M. (1975). Detection of specific sequences among DNA fragments separated by gel electrophoresis. J. Mol. Biol. *98*, 503–517.

Srivastava, D. (1997). Left, right . . . which way to turn [news, comment]? Nat. Genet. *17*, 252–254.

Steffen, W., Fajer, E.A., and Linck, R.W. (1994). Centrosomal components immunologically related to tektins from ciliary and flagellar microtubules. J. Cell Sci. *107*, 2095–2105.

Steffen, W., and Linck, R.W. (1988). Evidence for tektins in centrioles and axonemal microtubules. Proc. Natl. Acad. Sci. USA *85*, 2643–2647.

Steffen, W., and Linck, R.W. (1989). Relationship between tektins and intermediate filament proteins: an immunological study. Cell Motil. Cytoskeleton *14*, 359–371.

Stephens, R.E., and Lemieux, N.A. (1998). Tektins as structural determinants in basal bodies. Cell Motil. Cytoskeleton *40*, 379–392.

Stephens, R.E., Oleszko-Szuts, S., and Linck, R.W. (1989). Retention of ciliary ninefold structure after removal of microtubules. J. Cell Sci. *92*, 391–402.

Takada, S., and Kamiya, R. (1994). Functional reconstitution of *Chlamydomonas* outer dynein arms from alpha-beta and gamma subunits: requirement of a third factor. J. Cell Biol. *126*, 737–745.

Tilney, L.G., Bryan, J., Bush, D.J., Fujiwara, K., Mooseker, M.S., Murphy, D.B., and Snyder, D.H. (1973). Microtubules: evidence for 13 protofilaments. J. Cell Biol. *59*, 267–275.

Warner, F.D., and Satir, P. (1974). The structural basis of ciliary bend formation. Radial spoke positional changes accompanying microtubule sliding. J. Cell Biol. *63*, 35–63.

Wheatley, D.N. (1982). The Centriole: A Central Enigma of Cell Biology, New York: Elsevier Biomedical Press.

Wilkerson, C.G., King, S.M., and Witman, G.B. (1994). Molecular analysis of the gamma heavy chain of *Chlamydomonas* flagellar outer-arm dynein. J. Cell Sci. *107*, 497–506.

Witman, G.B. (1986). Isolation of *Chlamydomonas* flagella and flagellar axonemes. Methods Enzymol. *134*, 280–290.

Witman, G.B., Carlson, K., Berliner, J., and Rosenbaum, J.L. (1972a). *Chlamydomonas* flagella. I. Isolation and electrophoretic analysis of microtubules, matrix, membranes, and mastigonemes. J. Cell Biol. *54*, 507–539.

Witman, G.B., Carlson, K., and Rosenbaum, J.L. (1972b). *Chlamydomonas* flagella. II. The distribution of tubulins 1 and 2 in the outer doublet microtubules. J. Cell Biol. *54*, 540–555.

Witman, B., Wilkerson, C.G., and King, S.M. (1994). The biochemistry, genetics, and molecular biology of flagellar dynein. In: Microtubules, ed. J.S. Hyams and C.W. Lloyd, New York: Wiley-Liss, 229–249.

Wright, R.L., Salisbury, J., and Jarvik, J.W. (1985). A nucleus-basal body connector in *Chlamydomonas reinhardtii* that may function in basal body localization or segregation. J. Cell Biol. *101*, 1903–1912.

Young, R.A., and Davis, R.W. (1983). Yeast RNA polymerase II genes: isolation with antibody probes. Science *222*, 778–782.